Surface Dipole Layer Potential Induced IR Absorption Enhancement in *n*-Alkanethiol SAMs on GaAs(001)

Gregory M. Marshall,[†,‡] Gregory P. Lopinski,[§] Farid Bensebaa,[‡] and Jan J. Dubowski*,[†]

[†]*Department of Electrical and Computer Engineering, Université de Sherbrooke, Sherbrooke, Québec J1K 2R1, Canada,* [‡]*Institute for Chemical Process and Environmental Technology, National Research Council of Canada, Ottawa, Ontario K1A 0R6, Canada, and* [§]*Steacie Institute for Molecular Sciences, National Research Council of Canada, Ottawa, Ontario K1A 0R6, Canada*

The work function of *n*-alkanethiol self-assembled monolayers (SAMs) prepared on the GaAs(001) surface was measured using the Kelvin probe technique yielding the SAM 2D dipole layer potential (DLP). Direct *n*-dependent proportionality between the DLP values and the C−H stretching mode infrared (IR) absorption intensities was observed, which supports a correspondence of reported IR enhancements with the electrostatic properties of the interface. X-ray photoelectron spectroscopy is also used to verify the work function measurements. In addition, the principal components of the refractive index tensor are shown to be *n*-invariant in the ordered SAM phase. Our results suggest that a local field correction to the transition dipole moment accounts for the observed increase in IR activity through an increase to the electronic polarizability.

Introduction

Self-assembled monolayers (SAMs) are of technological interest as an integral component of functional interfaces. Prepared on the GaAs(001) surface, SAMs provide the opportunity to couple active molecular architectures to the sensitive electronic state of the semiconductor near-surface. Metal−molecule−semiconductor junctions[1−3] and sensor applications in the optical[4] and electronic domains are reported.[5−7] SAMs of long-chain *n*-alkanethiols have been investigated for their potential to form well-ordered and highly dense layers on GaAs(001) via thiolate chemisorption.[8−11] The SAM terminal groups may then be employed as functional chemical units. Important to their development is an understanding of the physical characteristics of these novel material systems, particularly with respect to the interface phenomena upon which device operation will ultimately depend.

Previously, Marshall et al.[12] reported on the observation of a 6× infrared (IR) absorption enhancement relative to the liquid phase of [HS−(CH$_2$)$_n$−CH$_3$] SAMs on GaAs(001). The enhancement was quantified in terms of an absorption coefficient, specific to the C−H stretching modes, derived from Beer−Lambert linearization of the IR absorbance over the methylene numbers *n* = 11−17.

Accounting for molecular surface orientation, density, and material phase (intrinsic) effects specific to both the liquid and polycrystalline states of alkane, ~3× of this enhancement was attributed to the electrochemical properties of the surface environment. Recently, Rosu et al.[13] reported on the dielectric constants of [HS−(CH$_2$)$_{15}$−CH$_3$] SAMs (*n*$_{15}$-SAMs) on GaAs(001) using IR ellipsometry. Our measurement of the absorption coefficient, cast in terms of the principal components of the refractive index tensor, is shown in the present work to accurately support the ellipsometry result and further, by virtue of the equivalence with our linearized result, suggests the low-frequency permittivity is *n*-invariant in the ordered SAM phase. Consequently, surface dipole related changes in the surface potential may be viewed as a variation of charge density or separation in an effective capacitor model.[14] That the monolayer density and order is of sufficient quality to validate the conclusion of invariance is supported by X-ray photoelectron spectroscopy (XPS) results used to characterize the SAMs over the methylene numbers in question; Nesher et al.[2] reported SAM thicknesses commensurate with the alkane chain length (i.e., < 15° chain axis tilt), and McGuiness et al.[9] reported surface coverages varying less than 12%. In addition, Marshall et al.[12] used C−H stretching mode component analysis to substantially fit the IR spectra over this regime using *n*-dependent linear scaling consistent with SAM variation in molecular length.

Despite these quantitative IR results, evidence for a unique physical mechanism explaining the enhancement phenomenon was lacking. Herein, we address this gap by demonstrating direct proportionality between the SAM vibrational absorbance and the surface potential of the corresponding 2D dipole layer measured using a Kelvin probe (KP). We argue the IR enhancement is determined by a functional relationship, specified by an increase in the electronic polarizability of the relevant transition dipole moments, which is due to the static field of the 2D dipole layer potential (DLP) illustrated in Figure 1. We discuss this in terms of a simple local field correction effect.

*Corresponding author. E-mail: jan.j.dubowski@usherbrooke.ca.

(1) Lodha, S.; Janes, D. B. *J. Appl. Phys.* **2006**, *100*, 024503.
(2) Nesher, G.; Vilan, A.; Cohen, H.; Cahen, D.; Amy, F.; Chan, C.; Hwang, J.; Kahn, A. *J. Phys. Chem. B* **2006**, *110*, 14363.
(3) Loo, Y.-L.; Hsu, J. W. P.; Willett, R. L.; Baldwin, K. W.; West, K. W.; Rogers, J. A. *J. Vac. Sci. Technol. B* **2002**, *20*, 2853.
(4) Ding, X.; Moumanis, K. H.; Dubowski, J. J.; Frost, E. H.; Escher, E. *Appl. Phys. A: Mater. Sci. Process.* **2006**, *83*, 357.
(5) Gartsman, K.; Cahen, D.; Kadyshevitch, A.; Libman, J.; Moav, T.; Naaman, R.; Shanzer, A.; Umansky, V.; Vilan, A. *Chem. Phys. Lett.* **1998**, *283*, 301.
(6) Wu, D. G.; Cahen, D.; Graf, P.; Naaman, R.; Nitzan, A.; Shvarts, D. *Chem.—Eur. J.* **2001**, *7*, 1743.
(7) Lee, K.; Lu, G.; Facchetti, A.; Janes, D. B.; Marks, T. J. *Appl. Phys. Lett.* **2008**, *92*, 123509.
(8) McGuiness, C. L.; Shaporenko, A.; Mars, C. K.; Uppili, S.; Zharnikov, M.; Allara, D. L. *J. Am. Chem. Soc.* **2006**, *128*, 5231.
(9) McGuiness, C. L.; Blasini, D.; Masejewski, J. P.; Uppili, S.; Cabarcos, O. M.; Smilgies, D.; Allara, D. L. *ACS Nano* **2007**, *1*, 30.
(10) Voznyy, O.; Dubowski, J. J. *J. Phys. Chem. C* **2008**, *112*, 3726.
(11) Voznyy, O.; Dubowski, J. J. *Langmuir* **2008**, *24*, 13299.
(12) Marshall, G. M.; Bensebaa, F.; Dubowski, J. J. *J. Appl. Phys.* **2009**, *105*, 094310.

(13) Rosu, D. M.; Jones, J. C.; Hsu, J. W. P.; Kavanagh, K. L.; Tsankov, D.; Schade, U.; Esser, N.; Hinrichs, K. *Langmuir* **2009**, *25*, 919.
(14) Cahen, D.; Naaman, R.; Vager, Z. *Adv. Funct. Mater.* **2005**, *15*, 1571.
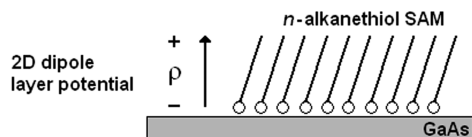
Figure 1. Illustration of the 2D dipole layer potential formed by a self-assembled monolayer (SAM) of *n*-alkanethiol on the GaAs-(001) surface.

Similar IR enhancements have been observed in other systems. In the work described by Dumas et al.[15] and Persson et al.,[16,17] the adsorption of CO on metals such as Ag and Cu is associated with a reduction in work function, electron donation to the metal from a relevant molecular orbital (MO), and a 4× increase in IR absorption intensity. In this case, however, overlap of the MOs with the metal Fermi level (FL) sensitizes them with respect to their occupation in what is referred to as back-donation. In this scenario, C−O bond stretching modulates the 2π-antibonding MO energy resulting in a dynamic oscillation of charge between the MO and the metal, effecting an enhancement of the vibrational polarizability. We contrast our results with this type of phenomenon on the grounds that the LUMO of the SAM−GaAs system should be well above the surface FL of the GaAs substrate.[2] Instead, we favor a change in the electronic polarizability as determined by the static dipole field. Moreover, the theoretical electrostatics of *n*-alkanoic monolayers at the air−water interface studied by Taylor and Bayes[18] suggest that an increase in local permittivity results from depolarization of the methyl moments in the static field of a 2D molecular array, effecting a reduction in the surface dipole. Our results concur, in general, with some discrepancies to be discussed. More importantly, this work highlights the intimate connection between the surface potential and dielectric constants of an adsorbed monolayer, with strong implications for the IR absorbances.

In determining the *n*-dependent 2D-DLP values from KP measurements, the contact potential difference (CPD) with respect to a Au reference probe is made. The CPD measures the relative work function difference from the FL to the vacuum level (VL). In doing so, both the internal potential associated with the space charge region, i.e., the band-bending potential, and the surface electron affinity (EA) are implicit in the data. In order to obtain the DLP, which is characteristic of the EA, the internal potential must be accounted for. Note that changes in the FL of GaAs have been observed by surface adsorption in other systems.[19] However, reports on the electronic passivation of thiol−GaAs(001) interfaces have indicated a null effect in terms of a repositioning of the surface FL with respect to the band edges, i.e., strong pinning applies. This may be due to the incommensurate surface density of the SAM with respect to the (001) surface[9] or due to the Ga-rich stoichiometry that is typically formed after the etching procedures required to prepare the surface for solution-based processing.[20] The absence of a surface FL shift was concluded in the landmark paper on sulfides passivation of GaAs by Lunt et al.[21] using time-resolved photoluminescence (PL) with

short-chain thiols and is corroborated by McGuiness et al.[22] using Raman scattering techniques with long-chain SAMs. Consequently, under the conditions of strong pinning effects, we are free to use the CPD as a measure of the *n*-variation of the DLP with the internal potential assumed fixed. Equivalent CPD results are verified on semi-insulating (SI) material and n⁺-type GaAs, suggesting that molecular induced band-bending interference is negligible. Moreover, FL pinning allows us to baseline the internal potential using appropriate reference surfaces in order to establish the absolute value of the DLPs. Independent verification of the DLP for n_{15}-SAMs is provided by XPS analysis of the relevant photoelectron binding energy shifts.

Experimental Details

Sample Preparation. Details on the preparation of *n*-alkanethiol SAMs ($n = 11, 13, 15, 17$) and those related to the recording of transmission IR data are described elsewhere.[12] Briefly, clean native GaAs(001) wafers (undoped SI or n⁺-type, Si-doped at 1×10^{18} cm⁻³) were oxide etched in 28% NH_4OH/H_2O and transferred under ethanol to 1−3 mM ethanolic thiol solutions, where the ordered SAM forms after 20 h incubation. Note that SI-GaAs samples were prepared on polished double-sided wafer to promote IR transmission mode analysis. As a result, an intensity factor of 2 is carried in the IR data. This improves the signal-to-noise ratio and is accounted for in computations where required.

Disordered monolayer reference surfaces were induced by postprocess immersion of n_{15}-SAMs in isopropanol (IPA) at 55 °C for 1 min, transferred directly from the ethanolic thiol solution without a rinsing/drying step. The added heat provides the necessary conformational energy required to disrupt the molecular order. Disordering was used to help provide a baseline for CPD referencing as described below. Consider that in the ideal SAM disordering without surface desorption may be counter-intuitive. However, local variation from this ideal may allow the SAM to disorder in the manner described. For example, McGuiness et al.[9] report domain boundaries of the order 10 nm in long-chain SAMs. Note that at 55 °C we do not expect significant surface desorption to occur for S-GaAs bond energies, which are reported to be in excess of 40 kcal/mol.[23] Note also that in molecular dynamics (MD) simulations of n_{15}-SAMs on Au by Hautman and Klein,[24] desorption is not factored into their calculations of the temperature-dependent increase in conformational disorder below 400 K. Dubois and Nuzzo provide corresponding IR spectroscopy data that track the MD results closely.[25] We do not see substantial evidence of surface desorption in our XPS results (see Supporting Information, section A).

Kelvin Probe Measurements. The KP instrument (KP Technology Ltd.) records the CPD with respect to a noncontact vibrating Au reference probe. Single point measurements were made using a 2 mm probe diameter and front/back surface grounding contact in air. CPD repeatability within ±20 mV was established based on results from five samples of n_{15}-SAM (see Supporting Information, section B). Electronic drift caused by stray capacitance was minimized with the use of a Faraday cage enveloping the KP unit. No absolute work function calibration was made.

X-ray Photoelectron Spectroscopy. XPS spectra were recorded in UHV ($< 10^{-8}$ Torr) with an Axis Ultra DLD (Kratos Analytical Ltd.) utilizing a monochromatic Al Kα source (1486.6 eV) and an analyzer pass energy of 20 eV. The analysis area (700 μm × 300 μm) was defined by an aperture in the transfer lens column. Photoelectron takeoff angles (ToA) were defined with respect to the surface normal by sample stage rotation.

(15) Dumas, P.; Tobin, R. G.; Richards, P. L. *Surf. Sci.* **1986**, *171*, 555.
(16) Persson, B. N. J.; Liebsch, A. *Surf. Sci.* **1981**, *110*, 356.
(17) Persson, B. N. J.; Ryberg, R. *Phys. Rev. B* **1981**, *24*, 6954.
(18) Taylor, D. M.; Bayes, G. F. *Phys. Rev. E* **1994**, *49*, 1439.
(19) Spicer, W. E.; Gregory, P. E.; Chye, P. W.; Babalola, I. A.; Sukegawa, T. *Appl. Phys. Lett.* **1975**, *27*, 617.
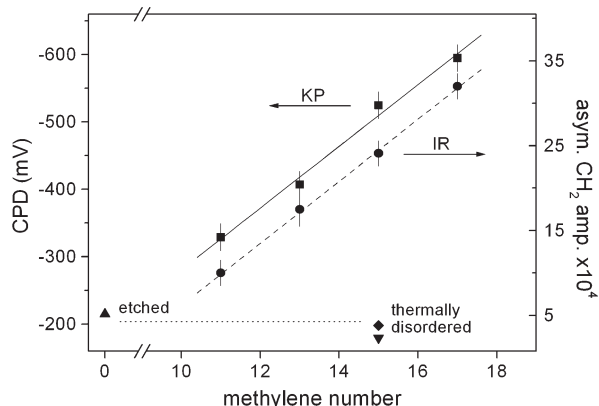(20) Aqua, T.; Cohen, H.; Vilan, A.; Naaman, R. *J. Phys. Chem. C* **2007**, *111*, 16313.
(21) Lunt, S. R.; Ryba, G. N.; Santangelo, P. G.; Lewis, N. S. *J. Appl. Phys.* **1991**, *70*, 7449.
(22) McGuiness, C. L.; Shaporenko, A.; Zharnikov, M.; Walker, A. V.; Allara, D. L. *J. Phys. Chem. C* **2007**, *111*, 4226.

(23) Voznyy, O.; Dubowski, J. J. *J. Phys. Chem. B* **2006**, *110*, 23619.
(24) Hautman, J.; Klein, M. L. *J. Chem. Phys.* **1989**, *91*, 4994.
(25) Dubois, L. H.; Nuzzo, R. G. *Annu. Rev. Phys. Chem.* **1992**, *43*, 437.

Figure 2. Kelvin Probe (KP) contact potential difference (squares) and infrared (IR) asymmetric CH_2 stretching mode peak absorbance (circles) vs chain length for [HS−$(CH_2)_n$−CH_3] SAMs on semi-insulating GaAs(001). KP etched only GaAs (up triangle). KP (diamond) and IR (down triangle) thermally disordered n_{15}-SAM. Baseline work function (dotted line).

Samples were electrically isolated such that the photoelectrons were referred to the vacuum level (VL). Binding energy reference to adventitious saturated hydrocarbon (285.0 eV) on an untreated GaAs wafer positioned the As $3d_{5/2}$ peak at 41.37 eV, which was subsequently used as a nominal calibration. No charge neutralization current was applied. Contrasted with this, uncorrected spectra at 0° ToA were measured from an etched (and reoxidized) GaAs reference surface and from a sample of n_{15}-SAM. These spectra were taken in charge neutralization mode, with an over-compensating thermionic current used in order to ensure minimal charging differences for the purpose of work function evaluation.

Peak fitting and quantification analysis were performed using the software package CasaXPS.[26] Symmetric (Voigt-type) or asymmetric (exponential-Voigt blend) line shapes were used to deconvolute the spectral envelopes into their constituent chemical states. Specific to the fitting of the S 2p and Ga 3s region, the irregular shape of the background of inelastic scattering in this region required a nonstandard approach since standard background functions did not apply satisfactorily. Consequently, an etched GaAs reference wafer was used to calibrate the background parameters (see Supporting Information, section C).

Interface Stability and Measurement Conditions. An important factor to consider in the preparation and measurement of the SAMs is the time stability of the interface. It is well-known these surfaces are limited by the extent to which the SAM provides a physical barrier to oxidative effects. For example, McGuiness et al.[8] reported that n_{17}-SAMs remain oxide free beyond 2 weeks as determined by XPS, while Nesher et al.[2] reported the stability of n_{11}-SAMs approaches 3 days. All samples were prepared in a N_2-purged glovebox and were transferred or stored under N_2 with measurements made in the initial condition immediately (IR, XPS) or well within the limiting time scales above (KP < 2 h). Specific to the KP results, it is understood that the disordered SAM may become partially reoxidized on a time scale less than that for the ordered SAMs. However, given the pinning conditions as described, and as later verified later using XPS, the disordered SAM provides a reasonable means to help baseline the internal potential of the GaAs surface permitting determination of the DLP magnitude.

Experimental Results

Kelvin Probe. The recorded CPD values (squares) are plotted upon the left axis in Figure 2 as a function of the alkane methylene number (*n*). The scale reference is the work function of the Au

probe at 0 mV. Also shown are the baseline CPD values of an etched but untreated GaAs reference (up triangle) and that from a sample of thermally disordered n_{15}-SAM (diamond). The (dotted) line between them forms the baseline CPD value approximating the GaAs work function without the SAM layer,[27] since the internal potential of the GaAs surface is considered constant according to the FL pinning effects as discussed in the Introduction. The linearization (solid line) of CPD values between n_{11} and n_{17} demonstrates the chain-length correspondence of the SAMs. The CPD changes at a rate 46 ± 3 mV/CH_2, more than twice that observed for *n*-alkanethiol SAMs on Au.[28,29] The results in Figure 2 were obtained on SI-GaAs material. Similar results (50 ± 4 mV/CH_2) were obtained on heavily Si-doped (n^+-type) GaAs material (see Supporting Information, section D). In line with the pinning model, slope equivalency between these two materials suggests there is no band-bending interference, i.e., no molecular induced change in the surface FL as a function of *n*. Note that we expect roughly 500 and 750 mV of band bending in the SI and n^+-type material, respectively, which equates to an order of magnitude variation in the occupancy of surface states. The latter estimate is based on well-known midgap pinning for n-type GaAs,[30] and the former is based on surface acceptor pinning near 270 meV above the valence band edge in undoped SI material.[31]

Infrared Spectroscopy. The IR results shown along the right axis of Figure 2 (circles) represent the peak absorbances of the asymmetric CH_2 stretching mode in a data set adapted from Marshall et al.[12] In that work, scale parametrization of the absorbance spectra by molecular chain length demonstrated a structural threshold for ordered self-assembly above the n_9-SAM value and linearization (dashed line) of the peak absorbance between n_{11} and n_{17} evaluated to an absorption coefficient (α) maximum of 3.5×10^4 cm^{-1} in a Beer−Lambert approach. Referring to the discussion of monolayer surface coverage above, a 12% variation over the methylene numbers n_{11} to n_{17} would result in only a 5% overestimate of the value of α derived from the linearization in Figure 2. Also shown in Figure 2 is the peak absorbance from a sample of n_{15}-SAM after thermal disordering (down triangle).

Representative IR spectra are provided in Figure 3, vertically shifted for clarity. The upper series illustrates the spectrum of C−H stretching modes from a sample of n_{15}-SAM. Identifying characteristics are the (a) CH_2 asymmetric mode near 2918 cm^{-1}, (b) CH_2 symmetric mode near 2850 cm^{-1}, and (c) the CH_3 mode associated with the terminal methyl group near 2960 cm^{-1}. The lower series represents the spectrum after thermal disordering. The loss of intensity is significant, at least 6× as expected based on the findings of our earlier report,[12] and is exacerbated by molecular reorientations more parallel to the surface on average; i.e., the orthonormal CH_2 transition moments are increasingly perpendicular to the optical field polarization, which is in the surface plane for transmission measurements. However, the reduction of IR signal is not attributed to significant material desorption loss as discussed above.

(26) Fairley, N. CasaXPS, Version 2.3.10, **1999−2005**.

(27) Implicit in the baseline assumption is that the interface dipole contribution from chemisorbed thiolate or oxide layers is approximately the same. Owing to the electronegative characteristics of both, it is expected these contributions increase the GaAs work function, the net equivalent effects of which are approximated in Figure 2. The CPD baseline is independently validated by XPS results.
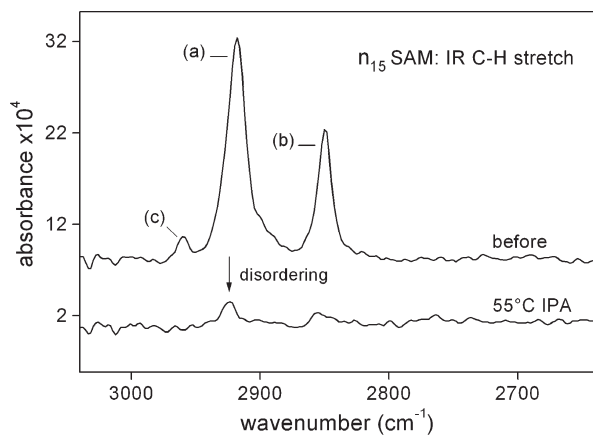
(28) Lü, J.; Eng, L.; Bennewitz, R.; Meyer, E.; Güntherodt, H.-J.; Scandella, L. *Surf. Interface Anal.* **1999**, *27*, 368.

(29) Howell, S.; Kuila, D.; Kasibhatla, B.; Kubiak, C. P.; Janes, D.; Reifenberger, R. *Langmuir* **2002**, *18*, 5120.

(30) Spicer, W. E.; Liliental-Weber, Z.; Weber, E.; Newman, N.; Kendelewicz, T.; Cao, R.; McCants, C.; Mahowald, P.; Miyano, K.; Lindau, I. *J. Vac. Sci. Technol. B* **1988**, *6*, 1245.

(31) Mandelis, A.; Budiman, R. A. *Superficies y Vacio* **1999**, *8*, 13.

Figure 3. C−H stretching mode IR spectra in transmission for n_{15}-SAMs before and after thermal disordering in 55 °C isopropanol (IPA). Reduction of intensity is due to molecular orientation and the loss of enhancement factors specific to the ordered SAM phase. See text for details.

X-ray Photoelectron Spectroscopy. Comparative As 3d spectra at 0° ToA are shown in Figure 4 from an etched and untreated GaAs reference surface (left) and from a sample of n_{15}-SAM (right). Under the FL pinning assumption and with the samples electrically isolated, use of an overcompensating neutralization current minimizes sample charging differences such that shifts in binding energy can be directly equated with the VL referenced increase in the FL, i.e., the reduction in EA associated with an outwardly directed sheet dipole layer, namely, the 2D-DLP magnitude. In Figure 4, the difference in the As 3d (uncorrected) binding energy positions associated with the GaAs phase measures 293 meV and reflects a decrease in the surface potential. The observed shift is commensurate with the change in potential one computes for the n_{15}-SAM (303 mV) by subtracting the CPD baseline from the linearization in Figure 2. We note that despite the uncertainties of using of KP surface photovoltage saturation techniques to determine the band-bending potential for GaAs particularly,[32] Aqua et al.[20] report an EA reduction of about 140 mV with respect to bare GaAs for nonanethiol (n_9-SAMs), which has some agreement with the trend derived from Figure 2 by baseline subtraction.

The S 2p core level XPS binding energy spectra are plotted in Figure 5 for thiolate in the surface environment of the ordered n_{15}-SAM (top panel) and in its disordered monolayer state (bottom panel). Separation of the S 2p doublet from the spectrum envelope proceeded systematically from the identification of GaAs photoelectron peaks and the background of inelastic scattering in an etched reference sample (see Supporting Information, section C). Three-point boxcar smoothing was applied (post-peak-fitting) in order to render the underlying chemical states more clearly. As prefaced in the Experimental Details, disordering does not result from any significant surface desorption, demonstrated qualitatively by the equal S 2p/Ga 3s intensity ratios observed in Figure 5. See Supporting Information, section A, for a discussion of the use of different ToAs, which is required in order to render the measurements equally surface sensitive due to the reduction of the attenuating overlayer thickness associated with the disordered SAM. The choice of ToAs also permits the constituent spectral components to be weighted in the deconvolution such that their peak shapes can be well resolved.

(32) Aphek, O. B.; Kronik, L.; Leibovitch, M.; Shapira, Y. *Surf. Sci.* **1998**, *409*, 485.

Table I. Correspondence of the IR Absorbance and 2D Dipole Layer Potential in [HS−(CH₂)ₙ−CH₃] SAMs on GaAs(001)

experiment	$n = 11$	$n = 17$	ratio
FTIR CH$_2$ asym str^a/×10^{-4}	9.9	31.8	3.2
ΔΦ by Kelvin probe/mV	119	394	3.3

^{a} Absorbance at asymmetric stretching mode peak.

Highlighted in Figure 5 is the positive binding energy shift observed for the S 2p core level in the SAM configuration. This shift is estimated to be +300 meV from the chemisorbed disordered state near 162.2 eV and demonstrates the change in surface potential associated with the SAM. A similar shift is observed for the C 1s data (see Supporting Information, section A). The increase in S 2p binding energy in the ordered SAM phase relative to the nominally referenced Ga 3s line is consistent with an increase in the VL referenced FL position and is corroborated by the As 3d results in Figure 4. Mutual agreement of the XPS results with the DLP for n_{15}-SAM supports the use of the CPD baseline to determine the DLP for the other n values, within an assumed tolerance of ±20 mV.

Discussion and Model Analysis

**Correspondence of the IR and 2D Dipole Layer Potential.** Based on the decreasing work functions relative to the baseline identified in Figure 2, the CPD values indicate that a sheet dipole or 2D dipole layer may be attributed to the SAM, with moments directed outward and with magnitude proportional to n. The net dipole moments are assumed to extend over the length of the molecule.[29] Together, the IR and CPD results demonstrate a strong linear variation, suggesting a sensitivity of the IR absorbance to the electrostatic surface environment of the SAM.

To further support the assertion of correspondence, the SAM CPD values are subtracted from the baseline CPD identified in Figure 2 in order to determine the surface potential contribution of each chain length, i.e., the 2D-DLP (ΔΦ). These are plotted in Figure 6 (circles) and fitted with a linear function. Comparison of the respective functions for the IR intensity and the DLP yields the empirical relation

$$I_{\text{IR}}(n) = \beta \Delta\Phi(n) + b \qquad (1)$$

with $\beta = 40 \times 10^{-4}$ V^{-1} and $b = 0.16 \times 10^{-4}$, in terms of volts (V) and dimensionless absorbance units (see Supporting Information, section E). The intercept (b) is negligible within experimental error, so we may conclude the IR intensity is *directly proportional* to the DLP (parametric in n). The observed direct proportionality means the two parameters scale at the same rate ($\sim 3 \times$), which is evident from the illustrative data example provided in Table I. Moreover, this scaling is greater than a unitary increase, which may be expected for the IR particularly, based on the change in absorption path length. Since the variation of IR intensity is linear in chain length, as is the DLP in the effective capacitor model (see eq 2), it is natural that these two observables will appear correlated when parametrized by n in eq 1. However, it is by virtue of the specific case of direct proportionality (characterized by the zero intercept) that we attribute the scaling of the enhanced IR intensity to a functional dependence based on the static field associated with the DLP. Correlation without a real physical dependence implied would be more likely to produce some other (nonequivalent) scaling, characterized by a different intercept. Details relating to the nature of the suggested effect are discussed in the last section.
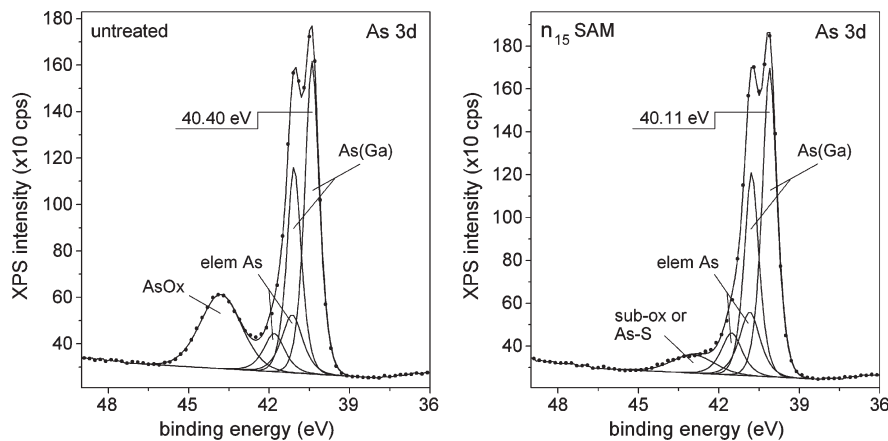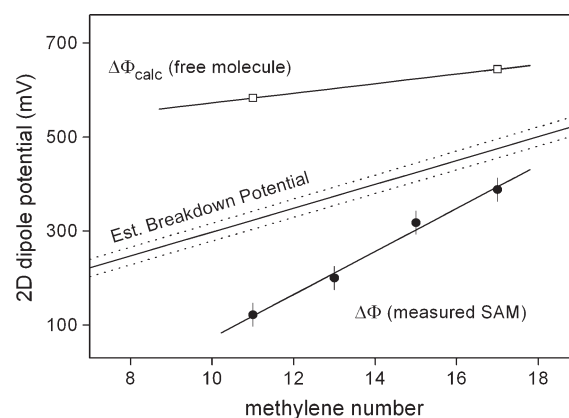
Figure 4. XPS core level As 3d spectra at 0° ToA from etched but untreated GaAs (left) and from GaAs prepared with n_{15}-SAM (right). Component peaks: As(Ga), bulk GaAs; elem As, surface or elemental As; AsOx, $As_2O_3 + As_2O_5$; subox or As−S, residual low oxidation states of As and/or As component of S-GaAs coupling. Doublets where indicated for 5/2 and 3/2 spin−orbit branching. Spectra are charge overcompensated and uncalibrated such that the binding energy reference indicates a change in potential corresponding to the DLP. See text for details.
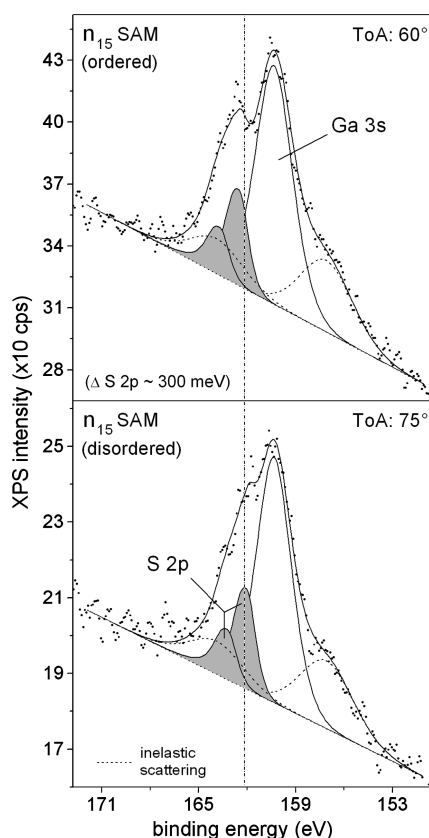
Figure 5. XPS core level S 2p/Ga 3s spectra of n_{15}-SAM before (upper) and after thermal disordering (lower). A relative binding energy shift of about 300 meV is observed for S 2p in the ordered SAM, indicating the change in work function corresponding to the 2D dipole layer potential. Spectra are nominally referenced to GaAs (Ga 3s at 160.3 eV) for convenience of comparison. Background of inelastic scattering is artificially assigned based on calibration to bare GaAs (see Supporting Information).

Effective Capacitor Model. Referring again to Figure 6, the calculated DLPs ($\Delta\Phi_{calc}$) are modeled (squares) based on noninteracting and surface-independent gas phase molecules according to

$$\Delta\Phi_{calc} = \frac{\sigma d}{\varepsilon_r \varepsilon_0} = \frac{\xi q d}{\varepsilon_r \varepsilon_0} = \frac{\xi \vec{\rho} \cdot \hat{z}}{\varepsilon_r \varepsilon_0} \quad (2)$$

Figure 6. Calculated 2D dipole layer potential (DLP) assuming known molecular dipole values in a SAM of noninteracting, surface-independent alkanethiols (squares). Measured 2D-DLP (circles) for chemisorbed SAM on semi-insulating GaAs(001). The breakdown potential is estimated based on the dielectric strength of polyethylene monolayers and the SAM molecular length.

where σ is the sheet charge density associated with the equivalent capacitor, d is the SAM thickness, ε_r and ε_0 are the relative and vacuum permittivities, ξ is the molecular surface density (5.2×10^{14} cm^{-2}) based on 4.24 Å alkane close-packing,[33] q is the elementary charge unit, $\vec{\rho}$ is the axial dipole moment per molecule (debye) based on quantum chemistry software results,[29] and $\hat{z}$ is the unit vector normal to the GaAs surface. Considering the permittivity values for polyethylene and *n*-alkanes,[34] a low-frequency limit of $\varepsilon_\gamma = 2.2$ is assumed. Implicit in eq 2 is the molecular length and the tilt angle of the molecular chain axis with respect to the surface normal. This value is reported to be 14° by near-edge X-ray absorption fine structure (NEXAFS)[8] and up to 19° by other means.[2,11,13] In our evaluations we assume that 14° applies, considering the high sensitivity of NEXAFS to bond orientation.

Also shown in Figure 6 is the dielectric breakdown potential of the SAM, estimated based on the molecular length and measurements of the dielectric strength (200 MV/m) of polyethylene

(33) Ulman, A.; Eilers, J. E.; Tillman, N. *Langmuir* **1989**, *5*, 1147.
(34) *CRC Handbook of Chemistry and Physics*, 70th ed.; CRC Press: Boca Raton, FL, 1989; pp E-53 and E-56.

Langmuir−Blodgett monolayers[35] and polypropylene thin films.[36] Surface-coupled molecular depolarization in dense SAMs of low polarizability (e.g., alkanes) has been referred to in the context of the cooperative molecular field effect (COMFE) proposed by Cahen et al.[14] Contrasted with SAMs of higher polarizability (e.g., systems of π-conjugated molecules), COMFE depolarization refers to the surface-coupled channel through which the SAM reduces the dipole field across itself, a field which can approach the critical limit of dielectric strength. The relations within Figure 6 bear this out illustratively and also concur with the findings of Taylor and Bayes,[18] in terms of an overall surface dipole reduction. However, for the *n*-alkanoic system they investigated, a saturation of the reduction effect based on methyl moment depolarization was calculated for chain lengths $n \geq 8$, since this effect was expected to be localized to the region including the first 3−4 methylene groups proximate to the methyl termination. In our system, we observed a reduction in the *absolute* surface dipole compared to the model based on non-interacting molecules but an increase in *relative* potential in the regime n_{11} to n_{17}. This distinction may be owing to the net effects of depolarization, namely covalent surface bonding that was not a factor in the Taylor and Bayes study.[18]

It should be noted that molecular dipole changes resulting from the excess valence charge density carried on chemisorbed thiolate (R-S:GaAs) with respect to the free thiol state (R-SH) upon formation of a covalent bond are unknown explicitly. The resulting surface complex will form its own interface dipole (inward) that tends to increase the work function by virtue of the partial ionic character of the sulfide bond. With respect to the capacitor model in eq 2, which is based on a 2D array of free alkanethiols, correspondence to the measured DLP is less direct as a result, rendering the precise mechanism of any depolarization effect unresolved in Figure 6. However, one may consider that the strong *n*-dependence observed in Figure 6 is due to an electrostatic interaction between the interface dipole associated with the surface complex and the molecular dipole (outward) associated with the alkane + methyl termination. Particular in this regard may be an increase in the covalency of the S−GaAs bond due to a redistribution of charge in the surface complex, which could be interpreted from Figure 5, though we could not uniquely identify evidence of this separate from the overall work function change. Nonetheless, our interest here lies in the static field of the SAM once established. With respect to the critical dielectric limit discussed above, Figure 6 provides a qualitative view of the substantial magnitudes of the internal fields involved.

Principal Components of the Refractive Index. The principal components of the complex refractive index $\mathcal{N}_{i,i}$ compute from the dielectric tensor $\varepsilon_{i,j}$ such that $\sqrt{\varepsilon_{i,i}} = \mathcal{N}_{i,i} = \eta_{i,i} + i\kappa_{i,i}$ when $\varepsilon_{i,j}$ is diagonalized and are now derived from the value of the absorption coefficient $\alpha = 4\pi\kappa\nu$ cited in the Experimental Results. Since the normal coordinates of vibrational displacement (r_q) for the symmetric and asymmetric CH_2 stretching modes are mutually orthogonal and perpendicular to the molecular length axes, defined by the C−C−C backbone plane, we assume uniaxial absorption asymmetry, as found by Rosu et al.,[13] and define the optical axis in terms of the molecular coordinates with imaginary principal components $\kappa_{1,1} = \kappa_{2,2}$ and $\kappa_{3,3} = 0$. The equivalency of $\kappa_{1,1}$ and $\kappa_{2,2}$ results from the ±45° mixed twist orientation of the C−C−C plane about the molecular axis in a two-chain surface

cell,[9] a fact recently verified in structural modeling results.[11] Isotropy is assumed for the real part of $\mathcal{N}_{i,i}$ off-resonance. From linear dispersion theory in a resonant medium the complex refractive index is[37]

$$\mathcal{N}(\omega) = \sqrt{1 + \sum_m \left(\frac{g_m}{\omega_m^2 - \omega^2 + i\Omega_m\omega} \right)} \qquad (3)$$

where g_m is the generalized oscillator strength of the *m*th resonant mode at ω_m, with damping constant Ω_m. Assuming $\eta_\infty = 1.43$ in the off-resonance limit,[13,38] and by suitable choice of the values in eq 3, the values $\mathrm{Re}(\mathcal{N})$ and $\mathrm{Im}(\mathcal{N})$ may be evaluated resulting in a solution to the Kramers−Kronig relations. The choice of modal parameters (ω_m and Ω_m) followed similar component assignments reported elsewhere.[12,38] These were first used to reconstruct the spectrum of κ, i.e., the $\mathrm{Im}(\mathcal{N})$, which was approximated from the recorded IR spectrum of n_{15}-SAM in Figure 3 by normalization of the asymmetric CH_2 peak to the value $\alpha = 3.5 \times 10^4$ cm^{-1} determined from Beer−Lambert analysis (see Supporting Information, section F). The real part of the complex index $\mathrm{Re}(\mathcal{N})$ follows accordingly. Note that in these calculations the recorded transition moments (Γ) exist in the surface plane (x,y) for transmission mode IR, i.e., coplanar with the optical polarization field, and are transformed from the (principal) molecular coordinates according to

$$\begin{pmatrix} \Gamma_x \\ \Gamma_y \\ \Gamma_z \end{pmatrix} = R_z(\varphi) \begin{pmatrix} 1 & 0 & 0 \\ 0 & \cos(\theta) & -\sin(\theta) \\ 0 & \sin(\theta) & \cos(\theta) \end{pmatrix} \begin{pmatrix} \cos(\psi) \\ \sin(\psi) \\ 0 \end{pmatrix} \qquad (4)$$

where the angle ψ refers to the mixed twist orientation (±45°) of the C−C−C backbone plane about the molecular axis, θ refers to the molecular axis tilt assumed (14°) as above, and $R_z(\varphi)$ is a small rotation matrix about the surface normal such that $\Gamma_x = \Gamma_y$ consistent with uniaxial symmetry. Vectorized elements of the material dipolar response (k) may be written in terms of $3k_{iso}$ of the isotropic bulk medium[38] but are modified as follows using the transformation in eq 4

$$k_i = \frac{3}{2} k_{iso} \Gamma_i^2, \quad i = x, y, z \qquad (5)$$

where the factor 1/2 accounts for the mixed planar orientation of transition moments in the surface cell compatible with the absorption symmetry. Using eqs 4 and 5, the principal components of eq 3 were calculated and are illustrated in Figure 7.

In the work by Rosu et al.,[13] IR ellipsometry was used to determine the dielectric constants specifically for n_{15}-SAM, expressed similarly using oscillator strength representation. Using their formulation and reported parameters for $\varepsilon = \varepsilon' + i\varepsilon''$, cast in terms of the principal extinction coefficients $\kappa_{1,1} = \kappa_{2,2}$, with $\kappa = (1/\sqrt{2})[(\varepsilon'^2 + \varepsilon''^2)^{1/2} - \varepsilon']^{1/2}$ and the transformation in eq 4, equivalent extinction coefficients were found (see Supporting Information, section F). Not only does the correspondence between the ellipsometric (single *n*-value) and Beer−Lambert determinations of the optical constants demonstrate their mutual validity, but it supports that these constants are invariant with chain length in the ordered SAM phase, the latter results having been derived from a linear fitting over several values of *n*.

(35) Sorokin, A. V.; Bai, M.; Ducharme, S.; Poulsen, M. *J. Appl. Phys.* **2002**, *92*, 5977.

(36) Liufu, D.; Wang, X. S.; Tu, D. M.; Kao, K. C. *J. Appl. Phys.* **1998**, *83*, 2209.

(37) Fowles, G. R. *Introduction to Modern Optics*, 2nd ed.; Dover Publications: New York, 1975; p 159.

(38) Parikh, A. N.; Allara, D. L. *J. Chem. Phys.* **1992**, *96*, 927.
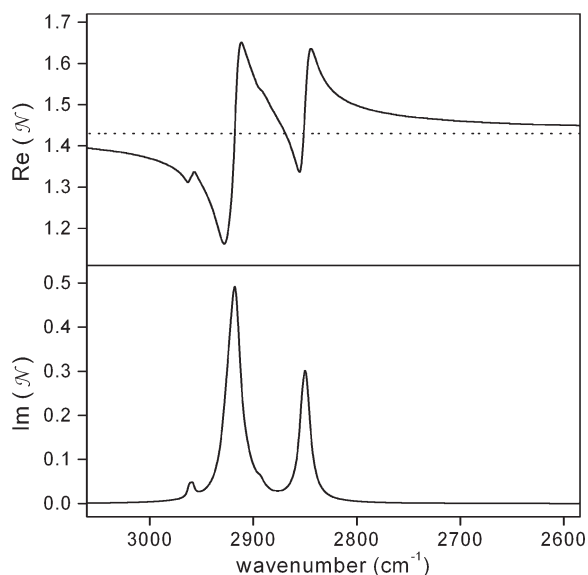
Figure 7. Calculated real (η) and imaginary (κ) parts of the refractive index $\mathscr{N}$ in terms of the principal components. Off-resonance isotropy (dotted line) with $\eta_{3,3} = 1.43$ is assumed. Uniaxial symmetry is applied such that $\eta_{1,1} = \eta_{2,2}$, $\kappa_{1,1} = \kappa_{2,2}$ and $\kappa_{3,3} = 0$ in the IR region defined.

The invariance of these constants also validates the underlying assumption that the SAMs are sufficiently dense and ordered over these methylene numbers, which suggests the low frequency permittivity ε_r is also *n*-invariant in the ordered SAM phase. In view of eq 2, this means that the DLP values may be regarded as a variation of charge density or separation in an effective capacitor model, not as a result of inconsistent permittivity that would result from inconsistent SAMs.

Note that the 3× extrinsic factor of IR enhancement can now be readily understood as an increase in oscillator strength. In eq 5, the vectorized dipolar response k for the SAM is expressed in terms of the effective magnitude k_{iso} and can be related to the real isotropic value measured in the liquid phase. Referencing the asymmetric CH_2 peak, the value of k_{iso} satisfying eq 5 for the SAM is $\kappa_{max}(\nu) = 0.66$. This computes to about 3.1× relative to the value measured from the liquid phase ($\kappa_{max}(\nu) = 0.15$), accounting for the intrinsic (polycrystalline) conformational and phase related increases, which are conservatively estimated to be about 40%.[12] The effective magnitude of k_{iso} satisfying eq 5 in the ellipsometry case is equivalent to our result for the SAMs as expected ($\kappa_{max}(\nu) = 0.68$).

Local Field Correction to the IR Transition Dipole. That the optical constants are *n*-invariant is critically important as stated. It justifies the assertion that the surface potential variation observed in Figure 2 may be represented in the effective capacitor model. Secondly, *n*-invariant permittivity suggests that the depolarization contribution described by Taylor and Bayes[18] may be less important here, its effects being highly localized as described above. Consequently, we are assured that the surface potential contribution of the SAMs is derived significantly from the dipolar molecular field, and we may now examine the correspondence between the IR enhancement and the DLP. This is expressed qualitatively in the following, discussed in terms of a local field correction to the IR transition dipoles in the SAM. The IR

absorbance is governed by the proportionality[39,40]

$$I_{IR} \propto \left| \vec{E} \cdot \frac{\partial \vec{\mu}}{\partial r_q} \right|^2 \qquad (6)$$

where $\vec{E}$ is the electric field vector of the IR optical field and the derivative is with respect to r_q defined above. The dipole moment $\vec{\mu}$ about the oscillator equilibrium is dynamically determined according to the average polarization density $\vec{P} = \vec{\mu} N$ near resonance ω_0 and consists of static dipole and vibrational contributions

$$\vec{\mu}_i(\omega) = \vec{\mu}_i(0) + \varepsilon_0 N^{-1} \sum_{j=x}^{z} (\varepsilon_{i,j}(\omega) - 1)\vec{E}_j(\omega) \qquad (7)$$

where N refers to the number density of C−H stretching modes and the indices now refer to the molecular coordinates. The frequency-independent term in eq 7 arises from the net molecular dipole, including the polarization due to local field contributions. Implicit in eqs 6 and 7 is that $\vec{\mu} = \vec{\mu}(r_q)$, with limits about the equilibrium position (r_{q0}) such that

$$\vec{\mu}(r_q)|_{0,\infty} = 0 \qquad (8)$$

and some maximum $\vec{\mu}(r_{qmax} \neq r_{q0})$ such that the derivative at r_{q0} is nonzero.[40] Molecular vibration is then considered a variance about r_{q0} in accordance with the phase value ωt along this derivative. Displacements of r_{q0} or changes to $\vec{\mu}(r_{q0})$ can result from perturbations of the electronic structure, changing the electronic contribution to the molecular polarizability. In the isotropic case, the values of $\vec{\mu}(r_q)$ are determined solely by the molecular structure with randomized orientations of the surrounding transition dipoles. In the SAM, proportionality of the DLP with the IR intensity in eq 1 suggests the local field contribution adds a substantial correction to the static polarization, manifesting as a vector-added component to $\vec{\mu}(r_{q0})_{SAM}$. Governed by the limits in eq 8 and our observation that

$$\left| \frac{\partial \vec{\mu}_{SAM}}{\partial r_q} \right|_{r_{q0}} > \left| \frac{\partial \vec{\mu}_{iso}}{\partial r_q} \right|_{r_{q0}} \qquad (9)$$

an increase to the oscillator dipole field in eq 7 is implied. In effect, our argument simply states that an increase in polarization results in an increase in polarizability. In the harmonic oscillator approximation, an increase in polarizability equates to a reduction in the force constant and a corresponding increase in resonant amplitude. This mechanism of IR enhancement is analogous to the Lorentz local field correction applied in standard nonresonant dielectrics,[41] in that the correction is local due to the macroscopic effect of a uniformly polarized medium.

Conclusions

The 2D-DLPs and corresponding IR absorbances of *n*-alkanethiol SAMs on GaAs(001) were shown to be highly correlated and in direct proportion. Comparison of the measured DLP values with both the capacitor model of the SAM and its estimated dielectric breakdown potential suggests that molecular depolarization effects may be realized upon coordination of the monolayer but that the internal field remains

(39) Allara, D. L.; Nuzzo, R. G. *Langmuir* **1985**, *1*, 52.
(40) Barrow, G. M. *Introduction to Molecular Spectroscopy*; McGraw-Hill: New York, 1962; p 80.

(41) Boyd, R. W. *Nonlinear Optics*; Academic Press: San Diego, 2003; p 177.

substantially high. The principal components of the SAM complex refractive index were then determined and expressed in terms of oscillator strength enhancement. The optical constants were found in agreement with published IR ellipsometry results confirming the *n*-invariance of the permittivity in the SAM regime, which reinforced the effective capacitor model. These facts support that the observed proportionality of the SAM vibrational absorbance with its surface potential may be understood in terms of a local field contribution to the transition dipole moment through an increase in the electronic polarizability.

Supporting Information Available: Angle-resolved XPS analysis of S 2p/Ga 3s ratio upon thermal disordering; CPD sampling series; background referencing in the S 2p/Ga 3s region; CPD of *n*-alkanethiol SAMs on n^+-type GaAs(001); correlation of IR intensity with the 2D-DLP; IR spectrum model and comparison with ellipsometric result. This material is available free of charge via the Internet at http://pubs.acs.org.